Journal of Orthopaedic Translation 45 (2024) 140–154

Contents lists available at ScienceDirect

Journal of Orthopaedic Translation

journal homepage: www.journals.elsevier.com/journal-of-orthopaedic-translation

Original Article

Enhanced articular cartilage regeneration using costal chondrocyte-derived scaffold-free tissue engineered constructs with ascorbic acid treatment

Kaiwen Zheng, Yiyang Ma, Cheng Chiu, Mengxin Xue, Changqing Zhang **, Dajiang Du *

Department of Orthopedic Surgery, Shanghai Sixth People's Hospital Affiliated to Shanghai Jiao Tong University School of Medicine, Shanghai, China

ARTICLE INFO

Keywords:
Articular cartilage regeneration
Cartilage tissue engineering
Costal chondrocytes
Osteochondral defect
Scaffold-free tissue engineering

ABSTRACT

Background: Cartilage tissue engineering faces challenges related to the use of scaffolds and limited seed cells. This study aims to propose a cost-effective and straightforward approach using costal chondrocytes (CCs) as an alternative cell source to overcome these challenges, eliminating the need for special culture equipment or scaffolds.

Methods: CCs were cultured at a high cell density with and without ascorbic acid treatment, serving as the experimental and control groups, respectively. Viability and tissue-engineered constructs (TEC) formation were evaluated until day 14. Slices of TEC samples were used for histological staining to evaluate the secretion of glycosaminoglycans and different types of collagen proteins within the extracellular matrix. mRNA sequencing and qPCR were performed to examine gene expression related to cartilage matrix secretion in the chondrocytes. In vivo experiments were conducted by implanting TECs from different groups into the defect site, followed by sample collection after 12 weeks for histological staining and scoring to evaluate the extent of cartilage regeneration. Hematoxylin-eosin (HE), Safranin-O-Fast Green, and Masson's trichrome stainings were used to examine the content of cartilage-related matrix components in the in vivo repair tissue. Immunohistochemical staining for type I and type II collagen, as well as aggrecan, was performed to assess the presence and distribution of these specific markers. Additionally, immunohistochemical staining for type X collagen was used to observe any hypertrophic changes in the repaired tissue.

Results: Viability of the chondrocytes remained high throughout the culture period, and the TECs displayed an enriched extracellular matrix suitable for surgical procedures. In vitro study revealed glycosaminoglycan and type II collagen production in both groups of TEC, while the TEC matrix treated with ascorbic acid displayed greater abundance. The results of mRNA sequencing and qPCR showed that genes related to cartilage matrix secretion such as Sox9, Col2, and Acan were upregulated by ascorbic acid in costal chondrocytes. Although the addition of Asc-2P led to an increase in COL10 expression according to qPCR and RNA-seq results, the immunofluorescence staining results of the two groups of TECs exhibited similar distribution and fluorescence intensity. In vivo experiments showed that both groups of TEC could adhere to the defect sites and kept hyaline cartilage morphology until 12 weeks. TEC treated with ascorbic acid showed superior cartilage regeneration as evidenced by significantly higher ICRS and O'Driscoll scores and stronger Safranin-O and collagen staining mimicking native cartilage when compared to other groups. In addition, the immunohistochemical staining results of Collgan X indicated that, after 12 weeks, the ascorbic acid-treated TEC did not exhibit further hypertrophy upon transplantation into the defect site, but maintained an expression profile similar to untreated TECs, while slightly higher than the sham-operated group.

Abbreviations: TEC, scaffold-free tissue-engineered construct; MSC, mesenchymal stem/stromal cell; ECM, extracellular matrix; Asc-2P, ascorbate 2-phosphate; CC, Costal chondrocytes; DMEM, Dulbecco's modified Eagle's medium; EDTA, ethylenediamine tetraacetic acid; RT-qPCR, Real-time polymerase chain reaction; GAPDH, glyceraldehyde 3-phosphate dehydrogenase; GAGs, glycosaminoglycans; DMMB, dimethyl methylene blue; PBS, phosphate-buffered saline; ICRS, International Cartilage Repair Society; ICRS-VHAS, ICRS Visual Histological Assessment Scale; H-E, Hematoxylin-Eosin; ANOVA, One-way analysis of variance; DEGs, differentially expressed genes; GO, Gene Ontology; KEGG, Kyoto Encyclopedia of Genes and Genomes; GSEA, gene set enrichment analysis.

* Corresponding author. Department of Orthopedic Surgery, Shanghai Sixth People's Hospital Affiliated to Shanghai Jiao Tong University School of Medicine, No.600 Yishan Rd, Shanghai, 200233, China.

** Corresponding author. Department of Orthopedic Surgery, Shanghai Sixth People's Hospital Affiliated to Shanghai Jiao Tong University School of Medicine, No.600 Yishan Rd, Shanghai, 200233, China.

E-mail addresses: zhangcq@sjtu.edu.cn (C. Zhang), dudajiang@sjtu.edu.cn (D. Du).

https://doi.org/10.1016/j.jot.2024.02.005
Received 11 November 2023; Received in revised form 29 January 2024; Accepted 20 February 2024

Conclusion: These results suggest that CC-derived scaffold-free TEC presents a promising method for articular cartilage regeneration. Ascorbic acid treatment enhances outcomes by promoting cartilage matrix production. This study provides valuable insights and potential advancements in the field of cartilage tissue engineering.
The translational potential of this article: Cartilage tissue engineering is an area of research with immense clinical potential. The approach presented in this article offers a cost-effective and straightforward solution, which can minimize the complexity of cell culture and scaffold fabrication. This simplification could offer several translational advantages, such as ease of use, rapid scalability, lower costs, and the potential for patient-specific clinical translation. The use of costal chondrocytes, which are easily obtainable, and the scaffold-free approach, which does not require specialized equipment or membranes, could be particularly advantageous in clinical settings, allowing for in situ regeneration of cartilage.

1. Introduction

Articular cartilage, a vital tissue that lines the ends of bones in joints, plays a pivotal role in facilitating painless and efficient movement. Trauma and chronic degeneration are key factors in articular cartilage deterioration, leading to joint pain and degenerative arthritis [1,2]. Given the limited capacity of articular cartilage for self-repair and regeneration, timely and appropriate intervention is crucial to prevent cartilage defects from progressing into the subchondral bone, which can lead to chronic joint pain, functional impairment, and reduced quality of life for affected individuals. Ultimately, joint replacement surgery may be required [3]. Autologous chondrocyte implantation and osteochondral transplantation offer treatment options but have limitations like limited graft sources and immunogenicity [3]. To tackle these challenges, tissue engineering has emerged as a promising field, providing innovative approaches for articular cartilage repair.

With the traditional tissue engineering paradigm of cells, signals, and scaffolds, the field of biomedical engineering has made great strides toward addressing clinical needs [4]. However, scaffold-based strategies raise concerns regarding the biocompatibility and degradation rate of the scaffolds, and potential immune responses [5]. In contrast, scaffold-free tissue engineering approaches have emerged as a promising alternative in the quest for solutions. In addition to avoiding the aforementioned potential issues associated with scaffolds, scaffold-free methods offer several advantages, including simplifying the manufacturing process, reducing costs, and the ability to generate high cell density structures. The underlying principle lies in that chondrocytes possess an innate ability to generate extracellular matrix, adhere to each other, and construct three-dimensional frameworks autonomously, without the intervention of external substances [4]. This process fosters cell–cell interactions and signaling and facilitates seamless integration with the host tissue upon implantation [6].

Previously, Ando et al. [7,8] developed a scaffold-free tissue-engineered construct (TEC) that was composed of mesenchymal stem/stromal cells (MSC) derived from synovium and an extracellular matrix (ECM) synthesized by the cells and confirmed its chondrogenic potential in vitro and in vivo. The fabrication of TEC simply depends on high cell density ($4.0 \times 10^5/cm^2$) and the presence of ascorbate 2-phosphate (Asc-2P) without any additional growth factors or special culture materials. The TECs can be gently detached from the culture dish after 14 days of culture while remaining intact. A further in-human pilot study using synovial-derived MSC-based TEC for cartilage repair in knee joints has shown that self-assessed clinical scores for pain, symptoms, activities, and quality of life were significantly improved at 24 months after surgery [9]. However, synovial-derived MSC-based TEC didn't show collagen type II production during fabrication in vitro unless a chondrogenic medium was added [7,8]. It brings uncertainty to the repair effect, as unfavorable differentiation may occur as a consequence of uncontrollable endogenous stimuli [10].

A critical impediment to articular cartilage repair lies in the limited cellularity and donor source constraints of articular cartilage. The proliferative limitations and dedifferentiation observed during monolayer expansion further hinder the therapeutic potential of articular chondrocytes [11]. Costal chondrocytes (CC), derived from the costal cartilage, are considered as an alternative cell source due to their superior proliferative capacity and the ability to maintain chondrogenic properties during in vitro expansion [12–15]. Crucially, CCs have an inherent capability to produce a hyaline cartilage-related matrix similar to articular chondrocytes [16–18]. This represents a significant advantage over MSCs that require in vitro induction, which can be inefficient and difficult to control accurately [19]. Additionally, CCs possess other distinct advantages such as abundant availability and low donor site morbidity [20,21]. The feasibility of using CC-derived pellets for articular cartilage repair was preliminarily validated in our previous experimental studies [22,23]. Due to limitations in oxygen and nutrient diffusion during the pellet culture, there are constraints on the size of the pellets to ensure the viability of central cells and the uniform distribution of extracellular matrix, which also limits its prospects for clinical application [4,24,25].

In this study, we propose a method for scaffold-free tissue engineering of cartilage using CC as seeding cells, under the condition of high cell density culture with the addition of only ascorbic acid. Comprehensive in vitro and in vivo investigations were conducted to evaluate the efficacy and translational potential of CC-TEC(Fig. 1). In vitro, CC-TEC constructs were fabricated to assess their structural characteristics, extracellular matrix secretion, and gene expression profiles. Using clinically relevant animal models, we evaluated the structural integrity, maintenance of functional cartilage properties, and seamless integration of the engineered tissue with surrounding native cartilage. These comprehensive evaluations provide valuable insights into the potential of CC-TEC as a clinically translatable solution with high promise for articular cartilage regeneration.

2. Methods

2.1. Isolation and characterization of costal chondrocytes

Rat costal chondrocytes were obtained from 10 to 12-week-old Sprague–Dawley rats following previously established protocols, as described in the supplementary file (Fig. S2) [26,27]. Briefly, the fresh rib cages were isolated using sterile scissors. Carefully removing the unwanted surrounding tissues, such as muscle and periosteum, from the costal cartilage using sterile surgical instruments. The costal cartilage samples were minced to 1 mm^3 and rinsed with sterile saline to remove any remaining debris or blood. To quantify the cell yield per unit weight, the harvested costal cartilage tissue was measured and documented. Transfer the cartilage pieces into a sterile dish. Add 1.5 mg/mL type II collagenase (Lot No.17101015, Gibco, US) in Dulbecco's modified Eagle's medium (DMEM, Lot No. SH30243.FS, HyClone, US) to the dish, ensuring that the cartilage samples are adequately submerged. The first step of digestion was carried out for 2 h at 37 °C and the second step of digestion was with 0.75 mg/mL type II collagenase in DMEM overnight. After the incubation period, the digested cartilage mixture was filtered with a 70 μm cell strainer and then transferred. Centrifuge the tube at 400 g for 5 min to collect the cell suspension. Carefully aspirate the supernatant, leaving only the cell pellet. Resuspend the cell pellet in a

growth medium (DMEM supplemented with 10% fetal bovine serum and 1% penicillin/streptomycin). The calculation method for determining the quantity of isolated cells is described in our previous study [15]. The quantification of chondrocytes obtained after digestion of a unit weight of cartilage was determined by comparing the measured number of chondrocytes with the previously obtained weight of the cartilage. The medium was changed every 2 days. Chondrocytes at 80–90% confluence were enzymatically detached using 0.25% trypsin/ethylenediamine tetraacetic acid (EDTA, Lot No.G4010-100 ML, Servicebio, China) and subsequently seeded onto fresh dishes at a consistent density. The cells were then cultured at 37 °C with 5% CO2. To determine the proliferation rate of cells across various passages (P0 to P5), we have calculated the population doubling time of cells at these different passages. The chondrocytes were seeded into 24-well plates, with 1×10^4 cells per well, and the experiment was conducted in triplicate. After 96 h, a cell counter (Cellometer Mini, Nexcelom, US) was used to count the cells, with trypan blue exclusion staining. The population doubling time (PDT) was calculated using the formula: PDT = t * lg2/(lgNt - lgN0), where N0 and Nt represent the cell counts after inoculation and t hours after culture, respectively. For the subsequent study, chondrocytes at passage 3 (P3) were selected.

2.2. Development of tissue engineering cartilage (TEC)

The development of TEC follows the previously established protocol [7,8]. Costal chondrocytes were firstly digested, counted, and seeded on 24-well plates at a density of 4.0×10^5 cells/cm^2. Within a day, the cells became confluent. Cells were cultured either in basic growth medium (named as ctrl group) or growth medium supplemented 0.2 mM L-Ascorbic acid 2-phosphate trisodium (Lot No. 49752, Sigma–Aldrich Inc., US, named as Asc-2P + group) and incubated at 37 °C in a 5% CO_2 incubator. The medium was changed every 2 days. On day 14, the cultured cells together with the ECM synthesized by the cells were detached from the plate by gentle pipetting. After being suspended in a growth medium for another 1 day, the detached complex was termed as a TEC.

2.3. Characterization of TEC

Cell morphology of TEC at 3, 7, and 14 days after seeding was captured by phase contrast microscope. Live/dead double staining was performed with a Calcein/PI Live/Dead Viability Assay Kit (Lot No. C2015S, Beyotime Biotechnology, China) following the manufacturer's instructions. Briefly, after the culture medium was removed, TEC was rinsed with sterile PBS and incubated with staining working solution at 37 °C for 30 min prevented from light. After incubation, the staining results were captured under a fluorescence microscope (Calcein AM emits green fluorescence, Ex/Em = 494/517 nm; PI emits red fluorescence, Ex/Em 535/617 nm). For the scanning electron microscopy (SEM) test, samples of TEC were firstly fixed in 2.5% glutaraldehyde in phosphate buffer. Following washing with PBS, the samples underwent dehydration through a series of ethanol solutions with increasing concentrations. The dehydrated TECs were frozen overnight at −60 °C and subsequently transferred to a vacuum drying oven (Alpha 2–4 LSCplus, Martin Christ Gefriertrocknungsanlagen, Germany) under a pressure of 0.105 Pa and at a temperature of −40 °C for a continuous duration of 24 h of freeze-drying process. The dried TEC samples were mounted on SEM stubs and subsequently coated with a thin layer of gold using a sputter coater. The SEM imaging was performed using a high-resolution SEM (Hitachi SU8010, Japan).

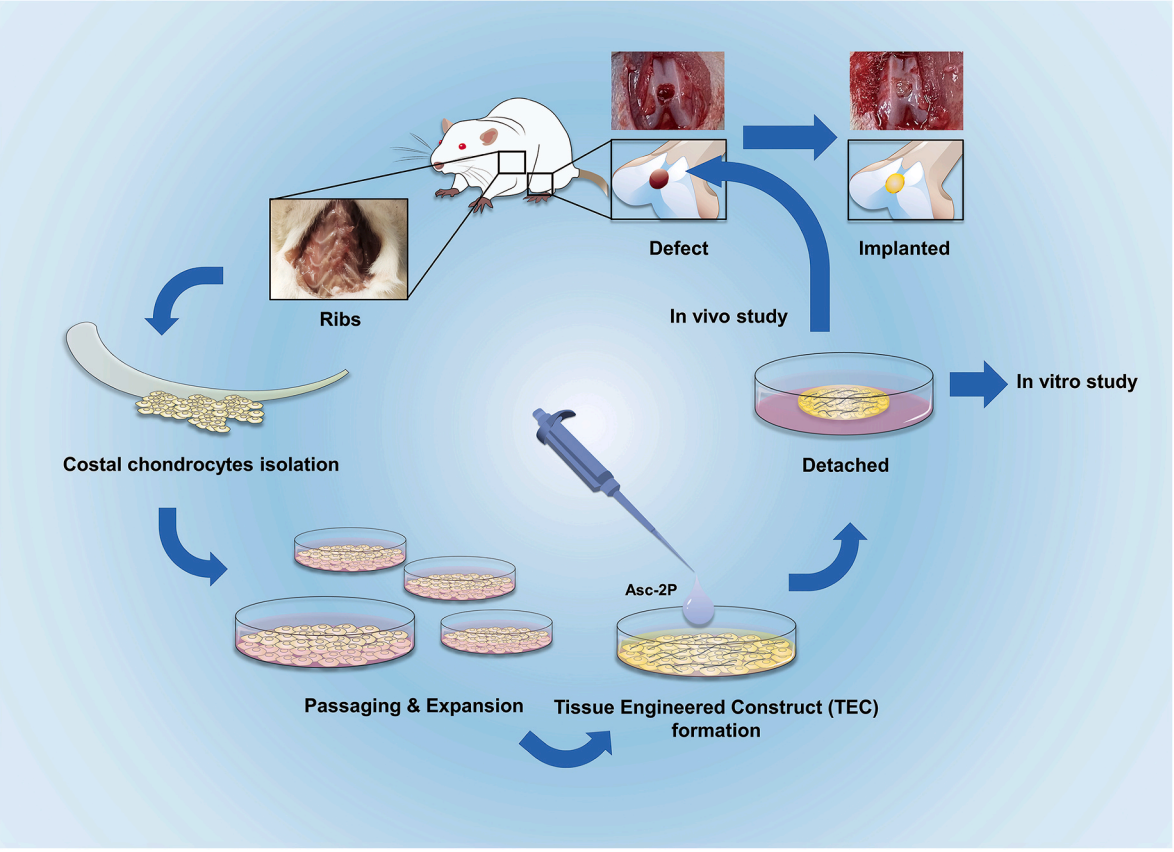

Figure 1. Schematic graph of this study. Costal chondrocytes were isolated to form a high cell-density tissue engineering construct with ascorbic acid treatment and were further investigated both in vitro and in vivo. Asc-2P: L-Ascorbic acid 2-phosphate trisodium.

2.4. RNA-sequencing and bioinformatics analysis

Total RNA was extracted from the experimental samples using the TRIzol reagent (Lot No. 12183555, Thermo Fisher Scientific Inc, USA) according to the manufacturer's instructions. The RNA amount and purity of each sample were quantified using NanoDrop ND-1000 (NanoDrop, Wilmington, DE, USA). The quality and integrity of the RNA were evaluated using the Agilent 2100 Bioanalyzer (Agilent Technologies, USA). High-quality RNA samples with RNA integrity numbers (RIN) above 7.0 were selected for subsequent library preparation. The cDNA library construction and RNA sequencing were operated by LC Bio-Technology CO., Ltd (Hangzhou, China) on the Illumina Novaseq™ 6000 platform. The obtained raw sequencing data were subjected to quality control using FastQC (http://www.bioinformatics.babraham.ac.uk/projects/fastqc/, 0.11.9) to assess the sequencing quality. Adapters and low-quality bases were filtered by Cutadapt (https://cutadapt.readthedocs.io/en/stable/, version:cutadapt-1.9). The clean reads were then aligned to the reference genome using HISAT2 (https://daehwankimlab.github.io/hisat2/, version:hisat2-2.2.1) package. Genes differential expression analysis was performed by DESeq2 software between two different groups. The genes with the parameter of false discovery rate (FDR) below 0.05 and absolute fold change ≥ 2 were considered differentially expressed genes. Differentially expressed genes were then subjected to enrichment analysis of GO functions and KEGG pathways. Bioinformatic analysis and visualization of data were performed using the OmicStudio tools at https://www.omicstudio.cn/tool.

2.5. Real-time polymerase chain reaction (RT-qPCR)

Individual qRT-PCR from additional replicate TEC samples harvested at day 7 and day 14 in each group validated the RNA-Seq results. The total RNA of TECs was extracted with an RNA Purification Kit (Lot No. B0004D, EZBioscience, US), and complementary DNA was prepared by using 4 × EZscript Reverse Transcription Mix II (Lot No.EZB-RT2GQ, EZBioscience, US) according to the manufacturer's instructions. RT-qPCR was performed in a volume of 10 μl. Complementary DNA was amplified using specific primers and SYBR Green Master Mix with QuantStudio™ 7 Flex real-time PCR System (Thermo Fisher Scientific, US). The amplification was performed under certain conditions: 5 min at 95 °C to activate, followed by 40 cycles, 15 s at 95 °C, and 60 s at 60 °C. RT-qPCR was performed under standard conditions and all experiments were performed in triplicate. The expression level of each gene was calculated using the $2^{-(\Delta\Delta CT)}$ method with glyceraldehyde 3-phosphate dehydrogenase (GAPDH) as the reference gene. Primers were synthesized by Tsingke Biotechnology Co., China, and sequences are shown in the supplementary file (Table S1).

2.6. Biochemical analysis

The secretion of glycosaminoglycans (GAGs) by the two groups of TECs was firstly assessed by alcian blue staining and semi-quantitatively compared by ImageJ software as previously described [28]. To further quantify the synthesis of GAGs, total GAGs were measured by the dimethyl methylene blue (DMMB) assay according to a previous protocol [23]. TECs from both control and Asc-2P + groups were digested in papain buffer containing5 mM L-cysteine(Lot No.168149, Sigma–Aldrich Inc., US), 200 μg/ml papain(Lot No.G8430, Solarbio, China), 0.1 M sodium acetate(Lot No.S5330, Solarbio, China) at 65 °C for 18 h and centrifuged for 5 min at 6000 rpm. Transfer an appropriate volume of the digested sample into a 96-well microplate. Add the DMMB reagent (Lot No.341088, Sigma–Aldrich Inc., US) to the sample and mix gently to ensure uniform distribution. Using a spectrophotometer (Varioskan LUX, thermofisher, US), measure the absorbance of the reaction mixture at a wavelength of 525 nm. Determine the GAG concentration in the samples by comparing the absorbance values with the pre-prepared standard curve of chondroitin sulfate (Lot No.T2980, Targetmol Chemicals Inc., US). DNA concentrations of TECs were assessed using a Helixyte™ Green Fluorimetric dsDNA Quantitation Kit (Lot No.17645, AAT Bioquest Inc, US) in accordance with the manufacturer's instructions. A standard curve was prepared by diluting the dsDNA standard provided in the kit using Tris–EDTA buffer. Each standard and sample was then added to separate wells of a 96-well plate. Subsequently, Helixyte™ Green working solution was added to each well and thoroughly mixed. The plate was incubated at room temperature for 2 min to allow for proper fluorescence development. DNA concentration was determined using the aforementioned spectrophotometer by measuring the fluorescence intensity at excitation/emission wavelengths of 490/525 nm and normalizing it to the dsDNA standard.

2.7. Animal experiments

Male Sprague–Dawley rats weighing between 250 and 300 g were used for this study after obtaining approval from the Animal Care and Use Committee of Shanghai Sixth People's Hospital (No. DWSY2022-0173). The rats were acclimated to the laboratory conditions for one week before the experiment. A total of 18 twelve-week-old male SD rats were randomly divided into three groups, with an additional 3 rats only receiving sham surgery as positive control. Each group consisted of 3 rats at each time point (6 weeks and 12 weeks), and bilateral knee surgeries were performed on them. Therefore, the sample size was $n = 6$ as it accounted for both left and right knees of the 3 rats in each group. After Anesthesia and sterilization, a longitudinal midline incision exposed the knee joint, allowing for careful dissection. Rats in the intact group referring to the sham surgery group which received no damage to the cartilage and had their wounds sutured. For rats in other groups, a microdrill was used to create a 1.5 mm diameter and 1 mm deep osteochondral defect in the tracheal groove. Saline irrigation was employed during drilling to prevent heat generation and maintain tissue hydration. In the blank group, rats remained untreated after the induction of osteochondral defects. Rats in the CC-TEC-Asc(−) group underwent TEC implantation which had been prepared devoid of ascorbic acid supplementation in advance and delicately positioned onto the defect sites within the knee joints of the rats. Conversely, rats assigned to the CC-TEC-Asc(+) group received implantation of TEC constructs that had been treated with ascorbic acid, a crucial component in the preparation. The joint capsule and skin were then closed. The rats were allowed to move freely in the cage after the operation. Rats were subjected to appropriate euthanasia before the dissection and harvest of distal parts of rat femur samples at 6 and 12 weeks after surgery for further analysis.

2.8. Nanoindentation tests

To examine the mechanical properties of the implanted tissue, nanoindentation tests were conducted according to a previously established protocol [29,30]. The distal parts of rat femur samples were harvested at 6 and 12 weeks after surgery and kept frozen at −20 °C until testing. To prevent sample dehydration, phosphate-buffered saline (PBS) was added to the testing area to maintain hydration throughout the entire duration of the tests. This ensured that the samples remained adequately moist during the nanoindentation experiments. For this experiment, we employed the BRUKER Hysitron TI 950 TriboIndenter, which was equipped with a Berkovich diamond probe. The instrument parameters were set to a maximum load of $V_{max} = 100$ μN, a maximum indentation time of $t = 2.5$ s, and a holding time of 2 s. The elastic modulus (E), hardness (H), and stiffness (S) of samples were determined using the Oliver-Pharr method, employing the TriboIndenter software provided with the equipment [30]. A total of 5 points on each sample were tested with an even distribution, and the average value of these measurements was considered as the representative result for each sample ($n = 6$).

2.9. Histological and immunohistochemical evaluation

TEC samples were fixed in 4% paraformaldehyde, dehydrated in a series of gradient sucrose-based solutions, and embedded in an Optimal Cutting Temperature compound (Lot No.4583, Sakura Finetek, USA). The embedded TEC blocks were sectioned into 10 μm slices using a cryostat. The rat femur samples were harvested and imaged by Leica S8 APO stereoscope and further quantitatively evaluated by the International Cartilage Repair Society (ICRS) macroscopic score (Table S2) [31]. Femur samples from each group were processed similarly to TEC samples, except that they were decalcified in 10% EDTA before embedding in paraffin and sectioning into 6 μm slices. Hematoxylin-Eosin (H-E), Safranin-O/Fast green, and Masson's trichrome staining were performed. Femur sections were further evaluated with ICRS Visual Histological Assessment Scale (ICRS-VHAS) and O'Driscoll score (Tables S3 and S4) [32,33]. To evaluate the production of collagen histologically, immunohistochemical staining was performed. Briefly, after deparaffinization, rehydration, and antigen retrieval using Tris–EDTA, sections were blocked with 0.1% Triton-X 100 and 3% BSA in PBS and then incubated with rabbit antibodies against collagen type I, II, and X (1:100, 1:100, and 1:50 respectively, Lot No.AF7001, AF0135, DF13214, Affinity Biosciences, China). Subsequently, TEC sections were incubated with Alexa Fluor® 488-conjugated Goat Anti-Rabbit IgG (H + L) (1:200, Lot No. GB25303, Servicebio, China) and IF555-phalloidin (Lot No.G1249-100T, Servicebio, China). At last, mount the coverslips on the section with an antifade mounting medium with DAPI. For femur sections, they were incubated with goat anti-rabbit secondary antibody conjugated with HRP (1:200, Lot No. S0001, Affinity Biosciences, China). The area of the immunocomplex was visualized by chromogen 3,3′-diaminobenzidine (DAB, Lot No.P0203, Beyotime, China). Fluorescent and bright field images were captured by a Leica DM6 digital microscope (Leica, Germany).

2.10. Statistical analysis

All histological scores were evaluated independently by three blinded observers. The data are presented as the mean ± standard deviation. Student's t-test was used for comparison between the two groups. One-way analysis of variance (ANOVA) coupled with Tukey's post hoc test was used to determine the significant differences in mechanical evaluation and histological scores among the groups. Bioinformatic analysis was performed using the OmicStudio tools at https://www.omicstudio.cn/tool. Other analysis results were visualized using Prism 8.0 software (GraphPad). A value of $p < 0.05$ was considered to indicate a significant difference.

3. Results

3.1. Morphological characterization and histological analysis of TEC

The cell yield of isolated chondrocytes was determined to be 2.31 ± 0.55 × 10^3 cells per milligram of cartilage tissue. There was no statistically significant difference in population doubling time of costal chondrocytes from P0 to P3, with average values of 34.8 ± 3.26, 29.18 ± 2.71, 30.73 ± 2.29, and 36.48 ± 2.77 h, respectively. However, a significant increase in population doubling time was observed for P4 to P5 costal chondrocytes, with values of 44.42 ± 4.15 and 59.67 ± 5.31 h,

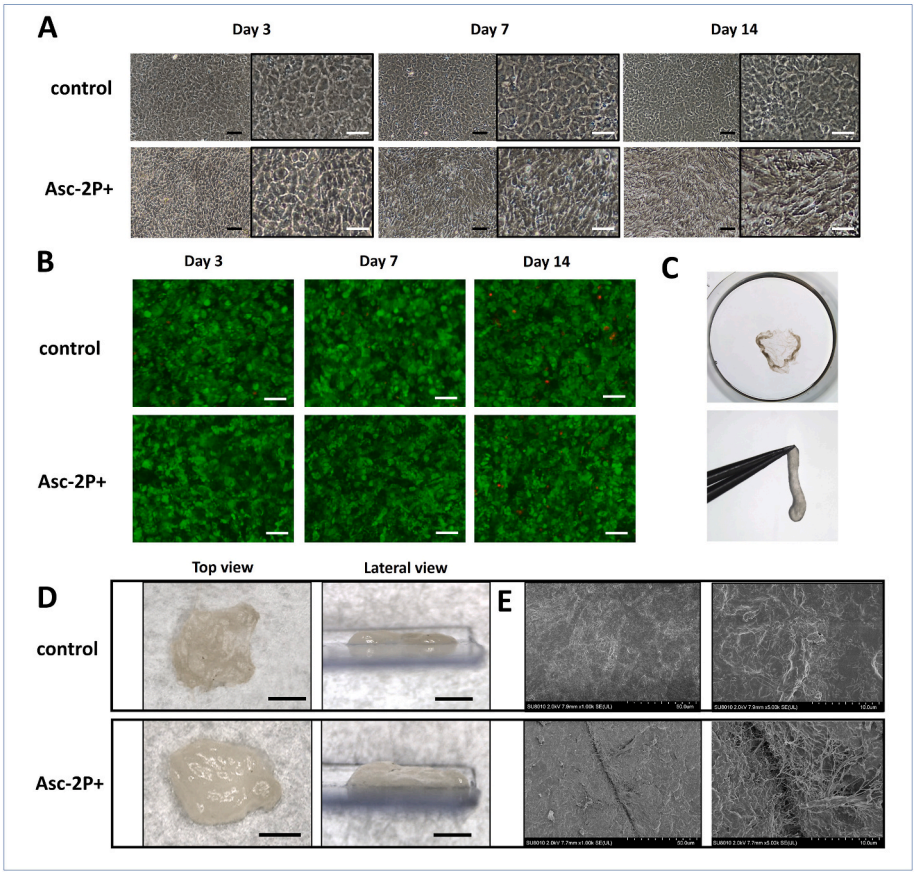

Figure 2. Characterization of TECs. A. Cell morphology at day 3, 7, 14. Black scale bar: 200 μm, white scale bar: 100 μm. B. Live/dead double staining of TECs. green: calcein AM, indicating live cells; red: propidium iodide, indicating dead cells. Scale bar: 100 μm. C. Gross view of TEC in the culture plate and when lifted. D. Gross view of TECs from the top and lateral sides. Scale bar = 1 mm. E. SEM images of TEC surfaces. Scale bar = 50 μm. (For interpretation of the references to color in this figure legend, the reader is referred to the Web version of this article.)

respectively, indicating a statistically significant difference compared to the cells from P0 to P3 (Fig. S1). The isolated costal chondrocytes exhibited a typical irregular polygonal morphology of chondrocytes and specifically expressed type II collagen (Fig. S2). Within 24 h after seeding, the costal chondrocyte was attached and showed high cell density. The morphology of cells changed differently under different culture conditions (Fig. 2 A). In the control group, the chondrocytes were closely arranged and maintained a polygonal shape until the 14th day. In the ascorbic acid-treated group, chondrocytes exhibited a gradual morphological change from irregular polygons to elongated fusiform. The cell viability did not decrease significantly within 14 days. It can be seen from the live-dead staining that despite the high cell density, most of the chondrocytes still maintained viability, and only a very small number of scattered chondrocytes died (Fig. 2 B). After detachment, TEC experienced a spontaneous process of contraction. The contracted tissue could withstand external forces such as surgical procedures and maintain its integrity (Fig. 2 C). After removing excess water on the surface, TEC presents a dense, opaque, smooth disk-like morphology with a certain thickness. It can be observed that the thickness of ascorbic acid-treated TECs was thicker than that of the control group, indicating that they contained more matrix components (Fig. 2 D). It can be seen that the fibers on the surface of the ascorbic

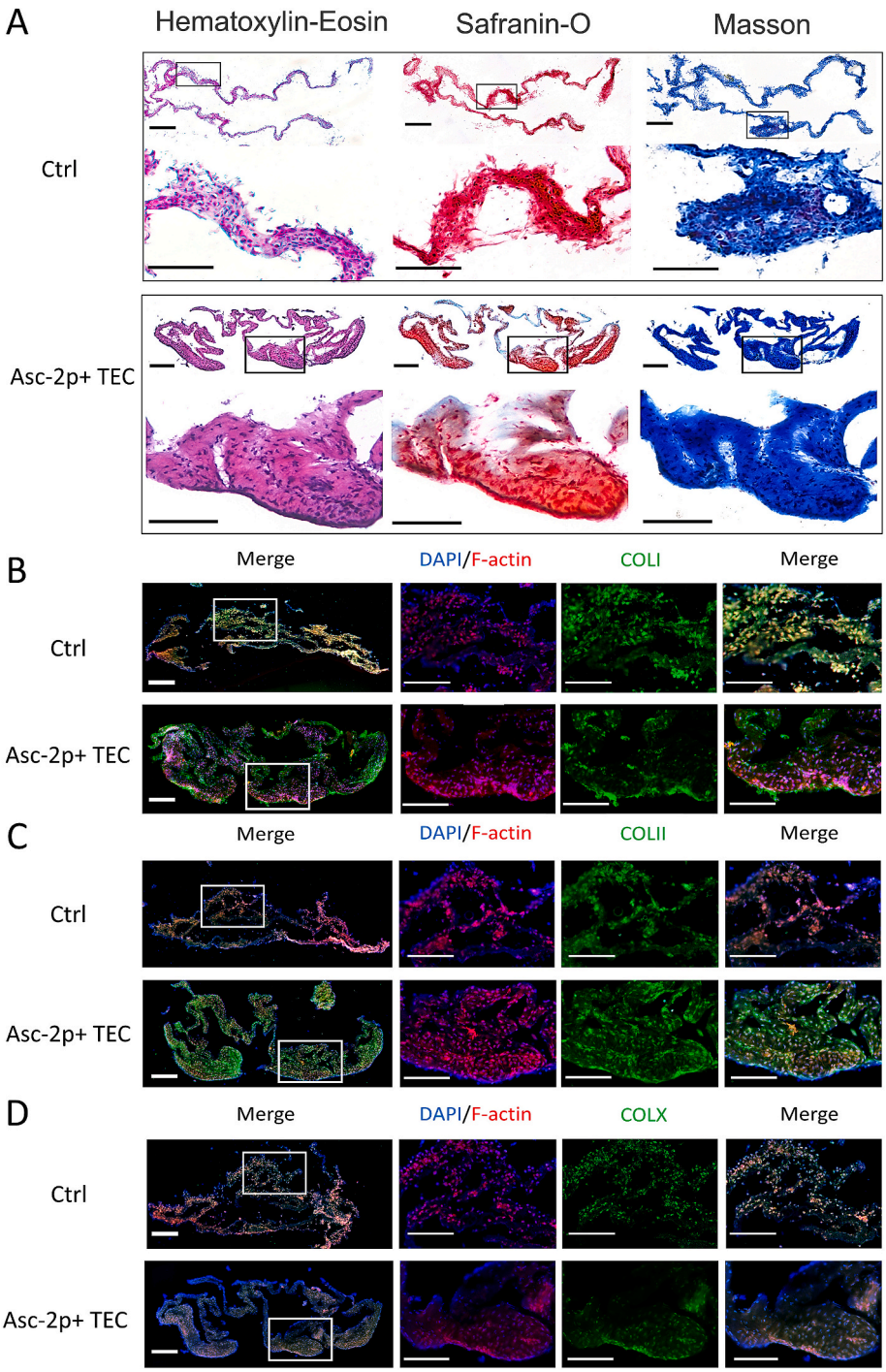

Figure 3. Histological analysis of TECs in two groups. A. H-E, Safranin-O, and Masson trichrome staining. B. Collagen type I, C. Collagen type II, and D. Collagen type X immunofluorescence staining. Scale bar = 100 μm.

acid-treated TEC were more abundant and intertwined intricately through the image of the TEC surface collected by the SEM (Fig. 2 E).

To explore the impact of ascorbic acid on the formation of TEC, TEC sections were stained after 14 days. Both groups of TECs displayed a high cell density. However, the control group exhibited thinner TECs with less pronounced matrix staining compared to the ascorbic acid-treated group (Fig. 3 A). Immunofluorescence staining revealed the presence of collagen types in both TEC groups. While both groups showed some positivity for collagen type I and type X, the signal for collagen type X was relatively weak, with no significant difference between the groups (Fig. 3 B, D). Remarkably, the ascorbic acid-treated TECs displayed a more homogeneous and widespread positivity for collagen type II (Fig. 3 C).

3.2. Gene expression analysis of TEC by RNA-seq and RT-qPCR

The results of the correlation coefficient analysis between samples indicate that there is a significant difference between the two groups of TEC, while there is high consistency within each group (Fig. S3). To identify differentially expressed genes (DEGs) between the two treatment groups, we applied a stringent statistical cutoff of $p < 0.05$ and $|\log2 \text{ fold change}| > 1$. A total of 1240 DEGs were identified, with 605 upregulated and 635 downregulated in ascorbic acid-treated TECs compared to the control (Fig. 4 C). The volcano plots and hierarchical cluster analysis showed the variation of mRNA expression between the control and ascorbic acid-treated TEC samples (Fig. 4 A). To explore the biological functions and pathways associated with the DEGs, we performed Gene Ontology (GO) and Kyoto Encyclopedia of Genes and Genomes (KEGG) enrichment analysis using clusterProfiler. GO enrichment analysis demonstrated DEGs were enriched in gene sets

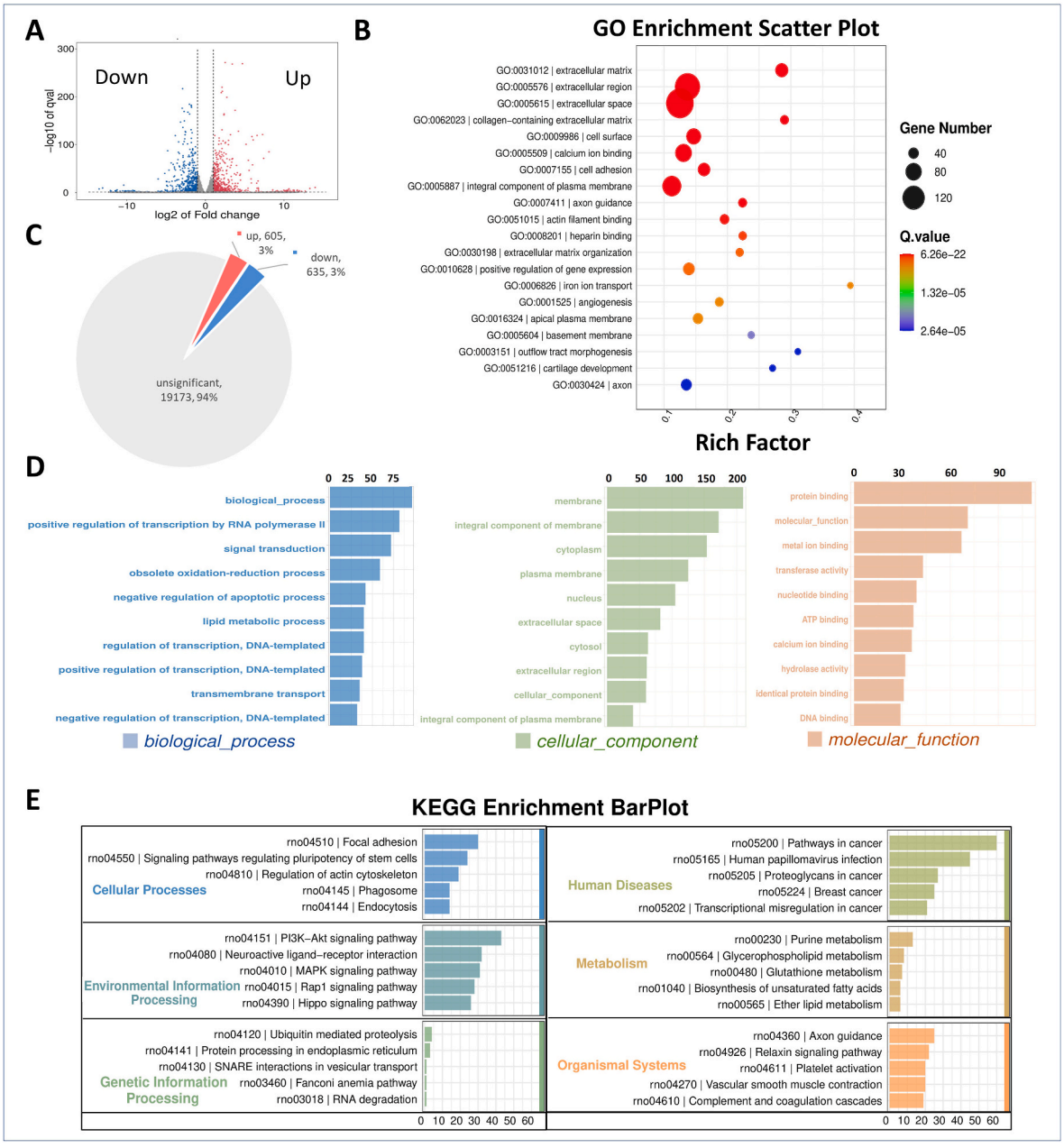

Figure 4. RNA sequencing analysis. A. A volcano plot illustrating differentially regulated gene expression from RNA-seq analysis between two groups. B. GO enrichment scatter plot. C. Pie chart of genes sequenced. D. GO functional clustering of DEGs. E. KEGG pathway classification. Asc-2p+: TECs treated with Asc-2P.

realated to extracellular matrix production, collagen-related matrix production, and cell adhesion (Fig. 4 B). GO classification results show that the terms "biological process"; "membrane" and "integral component of membrane"; "protein binding" were the most enriched categories of biological process, cellular component, and molecular function, respectively (Fig. 4 D). The KEGG database is used to determine the significant pathway of DEG. Several pathways were revealed including "Focal adhesion", "PI3K-Akt signaling pathway" and "Regulation of actin cytoskeleton" (Fig. 4 E). We also performed gene set enrichment analysis (GSEA) to identify the pathways and functions that were significantly enriched among the DEGs. The enriched gene sets included those related to fat metabolism, cell cycle, immune response, and chondrocyte differentiation. The top 30 enriched gene sets for GO and KEGG are shown in the supplementary file (Figs. S4 and S5).

The expression of selected genes related to cartilage matrix synthesis was represented by heat maps (Fig. 5 A, B). Validation of the RNA sequencing results was carried out using qPCR on selected DEGs related to cartilage matrix production. The qPCR results exhibited a high correlation with the RNA sequencing data, confirming the reliability of our transcriptomic analysis (Fig. 5 C). We evaluated the gene expression profile of TEC at both the 7-day and 14-day time points in our analysis. Selected cartilage production-related genes (Sox9, Col2a1, Acan) were all significantly elevated (all $P < 0.001$) in ascorbic acid-treated TECs compared to control TECs at both the 7-day and 14-day time points. However, regarding genes representing osteogenesis, the expression of Runx2 did not show significant differences at day 7 ($P = 0.09$), yet exhibited an increase at day 14 ($P = 0.04$). Additionally, the expression levels of Col1a1 were not statistically different at either time point ($P = 0.79$ and 0.13, respectively), whereas hypertrophic marker Col10a1 was upregulated significantly ($P < 0.001$).

3.3. GAG content analysis of TECs

To examine the effect of ascorbic acid on extracellular matrix

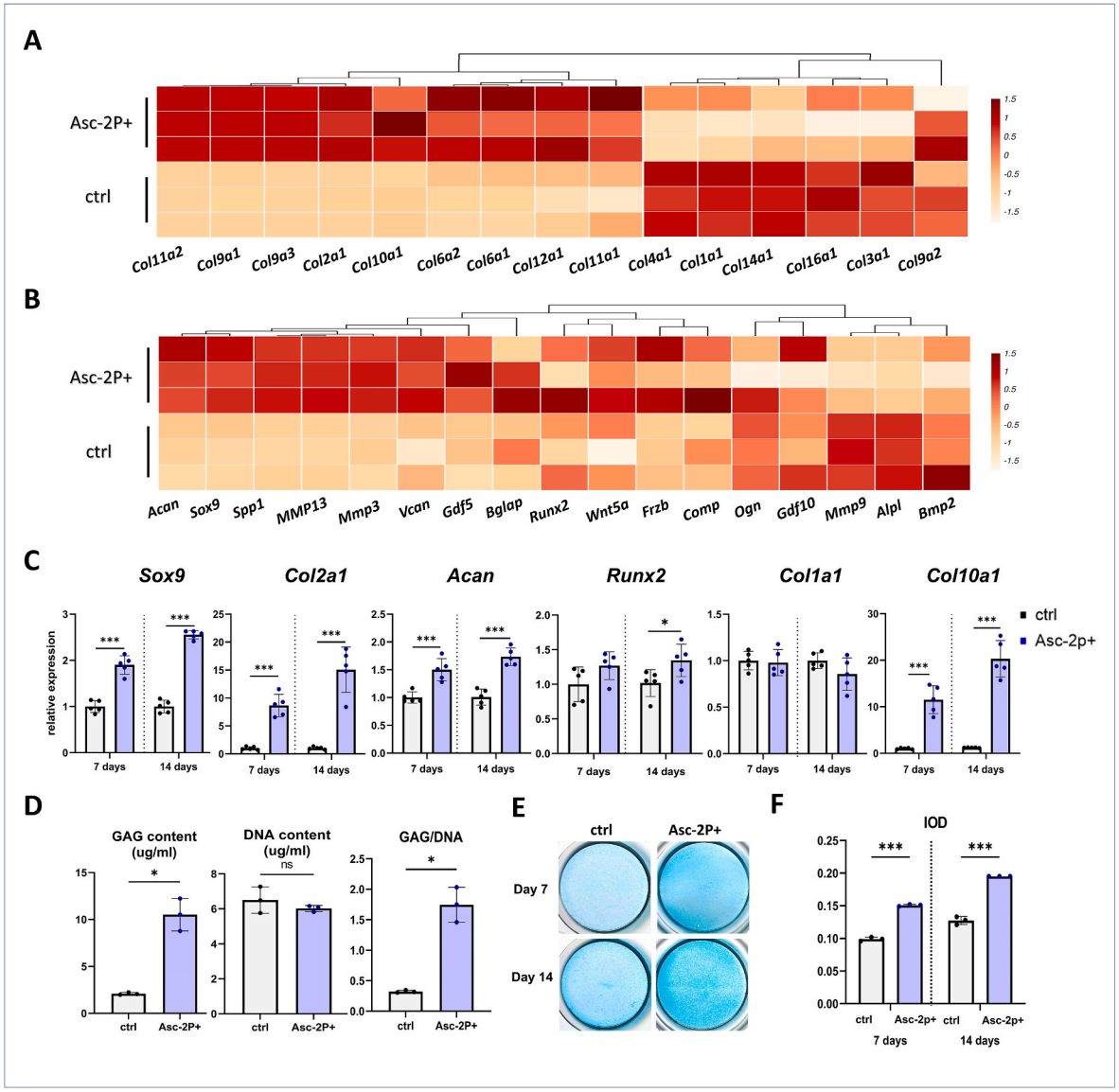

Figure 5. Gene expression analysis and biochemical analysis of TECs. A. Heat map of selected collagen-related gene expressions. B. Heat map of expressions of selected cartilage matrix-related genes (Acan, Sox9, Vcan, Comp, Frzb, Gdf5, Gdf10, Wnt5a), hypertrophy related genes (Mmp3, Mmp9, Mmp13, Alpl) and osteogenesis related genes (Bmp2, Runx2, Ogn, Bglap) between two groups. C. RT-qPCR validation results of selected genes within TECs at day 7 and 14(n = 5). D. GAG content, DNA content, and GAG/DNA ratio comparison between two groups(n = 3). E. Alcian blue staining of TECs in two groups and F. Semi-quantitative analysis of Alcian staining(n = 3). Asc-2P+: TECs treated with ascorbic acid; crtl: control TECs without ascorbic acid treatment. Significant letter: *, $P < 0.05$; **. $P < 0.01$; ***, $P < 0.001$. (For interpretation of the references to color in this figure legend, the reader is referred to the Web version of this article.)

synthesis, GAG contents were quantified. Ascorbic acid treatment significantly increased GAG production by TECs compared with untreated controls ($P = 0.013$), whereas DNA levels were similar between groups ($P = 0.386$) (Fig. 5 D). This suggested a substantial improvement in the matrix-forming capacity of chondrocytes, as reflected by the GAG/DNA ratio ($P = 0.013$). Alcian blue staining demonstrated enhanced GAG deposition in ascorbic acid-treated TECs than in control TECs at both 7 and 14 days, which was corroborated by semi-quantitative analysis of Alcian blue intensity (Fig. 5 E, F).

3.4. Macroscopic analysis of osteochondral defect regeneration in femur trochlear

During the surgery, the TECs were implanted into the defect site without additional fixation (Fig. 6 A). No animals developed infection or died until the end of the observation period, and no detachment of TECs from the implantation site was observed in the harvested specimens. Samples of the distal part of the femurs were collected and then imaged for macroscopic analysis (Fig. 6 C). It was observed that the articular cartilage defects in the blank group showed obvious indentations, which remained unfilled until 12 weeks. In contrast, the cartilage defects in both TEC-implanted groups were filled with white, shiny, opaque tissue, which was almost level with the surrounding cartilage. The fillers formed tight integration with the adjacent native cartilage, but the boundaries between them were still clear until 12 weeks post-surgery. No significant difference in gross appearance was noted between the two TEC-grafted groups. The macroscopic scores analysis conducted according to the ICRS guidelines consistently demonstrated results that are graphically represented in Fig. 6 B. The scores obtained for the TEC-implanted groups were significantly higher compared to the blank groups at both 6- and 12 weeks post-surgery. However, these scores remained significantly lower than those observed in the positive control groups. Notably, no statistically significant differences were detected between the two groups at both time point ($P = 0.20$ at 6 weeks and $P = 0.73$ at 12 weeks). Under stereomicroscopy, it was observed that the surface of the blank group samples collected at both time points exhibited irregular and rough features at the site of the cartilage defect (Fig. 6 C). In contrast, the surfaces of the grafts in both TEC-implanted groups appeared relatively smooth and even, resembling the morphology of the positive control group. Furthermore, this morphology was maintained for up to 12 weeks.

3.5. Nanoindentation tests of defect sites in femur trochlear

To evaluate the mechanical properties of the graft after transplantation, the nanoindentation experiment was performed (Fig. 6 D). The mechanical properties of samples in each group were quite different (Fig. 6 E). At week 6, the blank group showed the weakest hardness, elastic modulus, and stiffness properties, while the positive control group showed the significantly highest values. Samples from TEC-implanted groups showed mechanical properties between these two groups (Fig. 6 F). Ascorbic acid-treated TEC showed higher hardness and elastic modulus than control TEC after implantation ($P < 0.001$ and $P = 0.003$ respectively), although the stiffness reported no significant difference between them ($P = 0.18$).

3.6. Histological evaluation of femur trochlear

Samples were sectioned and stained for histological evaluation. Six weeks after surgery, the defect in the blank group was filled with irregular tissue, exhibiting a fibrous arrangement and lacking positive staining for Safranin-O and toluidine blue (Fig. 7 A). Immunohistochemical staining further revealed that the tissue was rich in type I and type X collagen but not type II collagen, suggesting that the repaired tissue forms fibrous tissue instead of cartilage tissue (Fig. 7 B). Both TEC implanted groups showed hyaline cartilage-like filling, in which it could be observed that the clustered chondrocytes were distributed in clearly defined lacunae embedded in the extracellular matrix (Fig. 7 A). Additionally, the staining for hyaline cartilage markers was visibly apparent and similar to the intact group. Immunohistochemical staining further confirmed the abundance of type II collagen and aggrecan in the matrix (Fig. 7 B). However, TECs that were not treated with ascorbic acid displayed a shallower staining for Safranin-O and type II collagen after transplantation compared to the ascorbic acid-treated TECs. These untreated TECs exhibited partial specificity in the staining for type I collagen, which was more intense than ascorbic acid-treated TECs. Positive staining for aggrecan was detected in the deep zones of the cartilage tissue, demonstrating its concentration in the territorial matrix and pericellular regions. Both groups showed similar secretion of type X collagen, displaying scattered specific staining. The positive staining was observed to be more widespread compared to the intact group, predominantly distributed in the pericellular matrix. Both ICRS and O'Driscoll histological scores came to the same conclusion, with the ascorbic acid-treated TEC transplant group being significantly better than the other two groups, but not as good as the intact group(Fig. 7 C).

At 12 weeks post-surgery, the defect sites in the blank group displayed subchondral bone remodeling; however, the surface was merely coated with a thin layer of fibrous tissue. Section staining results revealed negative staining for Safranin-O, type II collagen, and aggrecan within this tissue layer, while immunohistochemical staining indicated an abundance of type I collagen staining. These findings suggest that even after 12 weeks, the spontaneously repaired tissue failed to develop sufficient hyaline cartilage and instead was replaced solely by fibrous tissue (Fig. 8 A, B). TECs that were not treated with ascorbic acid maintained the content levels of GAG, type II collagen, and aggrecan in the matrix at 12 weeks post-implantation, as evidenced by safranin-O and immunohistochemical staining results. Ascorbic acid-treated TECs maintained a smooth and regular morphology on the joint surface at 12 weeks post-implantation, with abundant levels of GAG, type II collagen, and aggrecan in the matrix, as indicated by deeper staining. In contrast to the intact group, which displayed relatively shallow and localized distribution of both type I collagen and type X collagen, the staining intensity of these collagens in both the treated TEC group and the untreated TEC group was stronger(Fig. 8 A, B). However, upon comparing the staining patterns between the treated and untreated TEC groups, no discernible variations in the distribution patterns of type I collagen and type X collagen were observed. Both groups displayed similar IHC staining intensities and localization of these two collagen types within the cartilage tissue. This indicates that the ascorbic acid treatment did not induce any notable changes in the deposition or localization of these collagens in the study group compared to the control group. The histological scores at 12 weeks post-surgery were consistent with the results at 6 weeks, with the ascorbic acid-treated TEC transplantation group exhibiting significantly higher scores (Fig. 8 C).

4. Discussion

The emergence of tissue engineering techniques has shed light on articular cartilage regeneration. Classical tissue engineering techniques rely on the combination of cells, signals, and scaffolds [4]. However, the introduction of a scaffold into a tissue-engineered construct brings relevant concerns. Firstly, the long-term cytotoxicity and exposure of cells to the harsh processing requirements of scaffold-based constructs (e.g., spinner shear, elevated temperatures, toxic polymerizing chemicals), which leads to decreased cell viability must be considered [5,6]. Moreover, the biodegradability of incorporated biomaterials and the possibility of eliciting an immunological response also cannot be ignored [6,34]. Other scaffold-related concerns include complicated fabrication methods, issues with heterogeneous cell distribution or cell migration, stress shielding from mechano-transduction, and insufficient retention and integration with surrounding tissue [6,35–37]. To avoid the concerns mentioned above, scaffold-free tissue engineering seems to

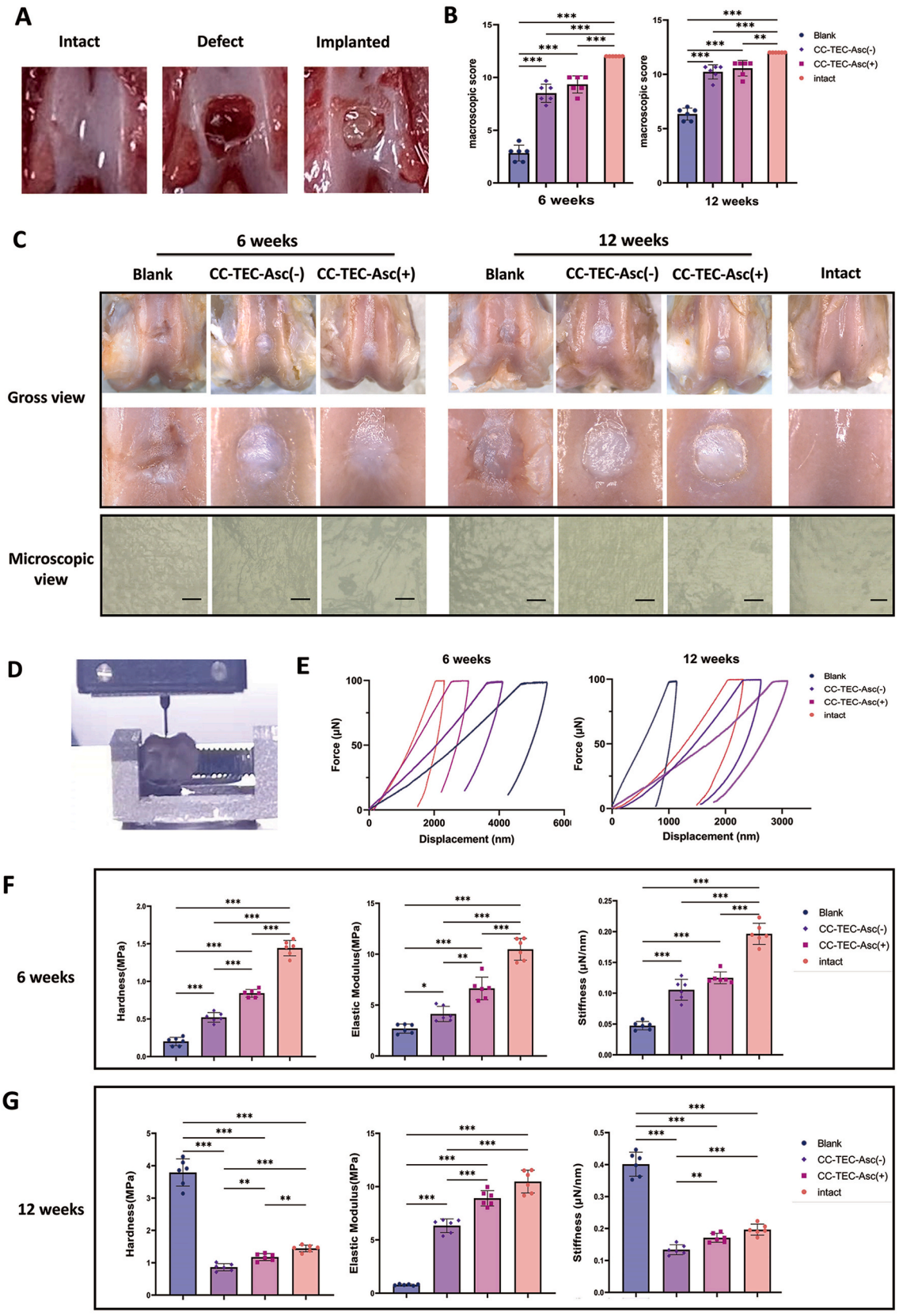

Figure 6. Macroscopic evaluation and nanoindentation tests for femur samples from four groups. A. TEC implantation during the surgery. B. ICRS macroscopic score analysis of four groups (n = 6). C. Macroscopic views of samples harvested from four groups. D. Nanoindentation tests for each sample with a special fixation device. E. Representative curves of nanoindentation tests. F-G. Analysis of experimental results of nanoindentation at 6- and 12-weeks post-surgery(n = 6). Scale bar = 50 μm; Significant letter: *, $P < 0.05$; **. $P < 0.01$; ***, $P < 0.001$.

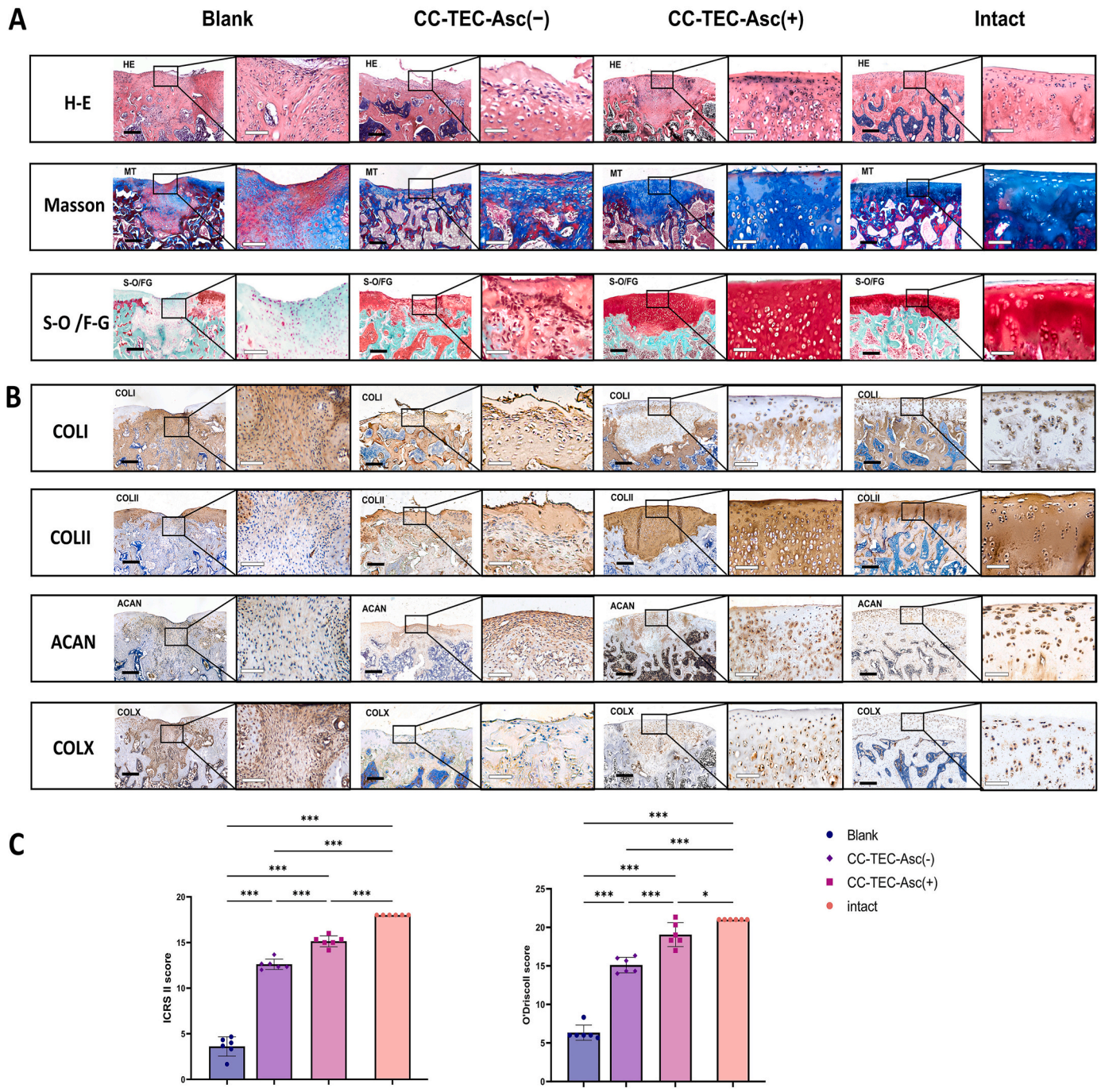

Figure 7. Histological and immunochemical staining of femur samples at 6 weeks post-surgery. A. H-E, Masson trichrome, and Safranin-O/Fast green staining. B. Immunochemical staining of collagen type I, II, X, and aggrecan. Black scale bar = 200 μm, white scale bar = 50 μm. C. Histological analysis using ICRS II and O'Driscoll score systems. CC-TEC-Asc(+) means groups in which rats received ascorbic acid-treated TEC implantation while CC-TEC-Asc(−) only received control TEC implantation. Significant letter: ***, $P < 0.001$. (For interpretation of the references to color in this figure legend, the reader is referred to the Web version of this article.)

be a viable alternative.

The formation of aggregate culture through centrifugation is a widely utilized technique in cartilage tissue engineering. In this approach, cell aggregates or pellets undergo chondrogenic differentiation within a three-dimensional structure. However, the presence of aggregates exceeding 500 μm in diameter poses challenges related to diffusion limitations and hypoxia within their cores [6,24,38,39]. Furthermore, even if micro-pellets are successfully formed and re-integrated, the nonuniformity at the boundaries and uneven distribution of the matrix within the integrated aggregates may impede their regenerative efficacy following implantation [40,41]. In this study, we utilized an approach depending on high cell density ($4.0 \times 10^5/cm^2$) and the presence of Asc-2P to fabricate a scaffold-free TEC as previously described [7,8]. Under this cell density, CC maintained high viability and cartilage-associated matrix production (Figs. 2B–Fig. 3 A). It could be easily detached by applying gentle shear stress using the pipette, and subsequently undergoing spontaneous contraction, which is consistent with previous reports [42]. The transformation of TECs from a monolayer complex to a three-dimensional structure is related to contractile forces generated within the actin-cytoskeleton [8,43]. The development

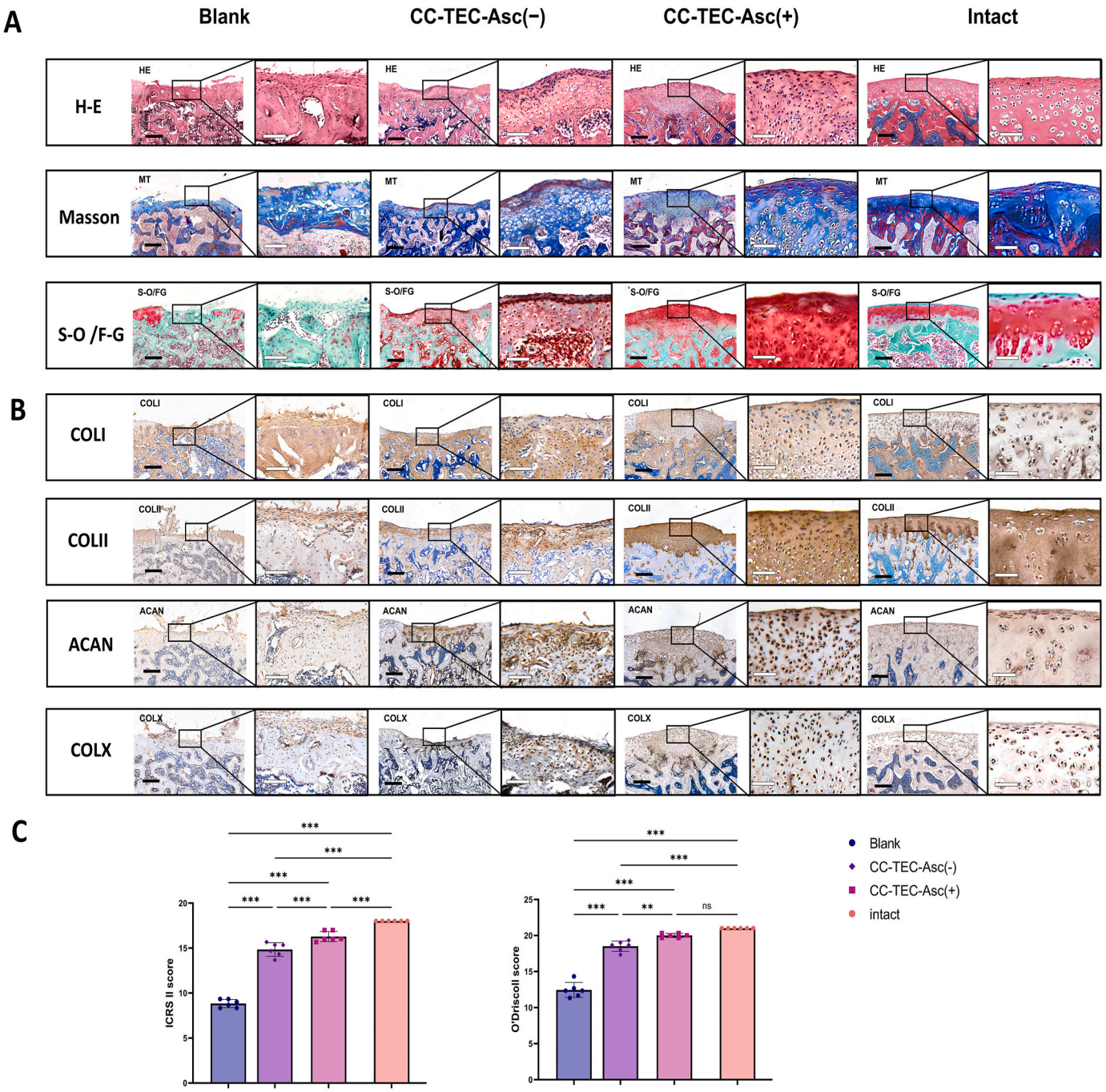

Figure 8. Histological and immunochemical staining of femur samples at 12 weeks post-surgery. A. H-E, Masson trichrome, and Safranin-O/Fast green staining. B. Immunochemical staining of collagen type I, II, X, and aggrecan. Black scale bar = 200 μm, white scale bar = 50 μm. C. Histological analysis using ICRS II and O'Driscoll score systems. CC-TEC-Asc(+) means groups in which rats received ascorbic acid-treated TEC implantation while CC-TEC-Asc(−) only received control TEC implantation. Significant letters: *, $P < 0.05$; ***, $P < 0.001$. (For interpretation of the references to color in this figure legend, the reader is referred to the Web version of this article.)

of TECs does not encounter size limitations, as their dimensions are determined by the container and can be formed in a single step, thereby avoiding the nonuniformity associated with secondary integration. Such characteristics significantly enhance the translational potential of TECs in clinical applications. An in-human pilot study has adopted large culture dishes up to 150 cm^2 to produce TECs whose size and thickness met the requirements of clinical translation (about 1.5 cm in diameter) and found significantly improved scores after surgery [9]. In addition, the presented approach does not require any special equipment or growth factor, thus simplifying the manufacturing process and reducing costs. This is particularly noteworthy as autologous chondrocyte implantation, which is known to have high costs, predominantly stems from the expenses associated with in vitro cultivation [10]. In contrast, techniques such as cell sheet formation usually require special cell culture equipment such as thermo-responsive systems [6,44,45]. Moreover, TECs are relatively stronger compared to chondrocyte sheets, which are generally fragile and thin, making construct handling difficult. Our study showed CC-derived TECs endured surgical procedures including trimming before transplantation without tearing down (Figs. 2C–Fig. 6 A).

Another advantage of TECs is their adhesion and integration to surrounding native cartilage. Integration is critical in cartilage regeneration as it provides stable biological fixation, load distribution, and the proper mechano-transduction necessary for homeostasis [46]. However, cartilage-to-cartilage integration is difficult to achieve because of its anti-adhesive characteristics and limited cell migration within it [41,47,48]. Studies have found the adhesive property of TECs to host tissue without any additional intervention [7,34]. In this study, we evaluated the adhesion and integration of CC-derived TECs by implanting them in an osteochondral defect model. All grafts stayed in situ with a smooth surface until week 12(Fig. 6 C). Histological results have shown that CC-derived TECs were integrated into the host cartilage without any apparent discontinuities from the superficial layer through to the deep layer (Figs. 7 and 8). Previous experiments have also reported the consistent characteristic of TECs adhering to knee joint cartilage defects without the need for sutures or auxiliary fixation agents [9,49]. These results are superior to those of CC-derived pellets studied in our previous experiment [23].

The effect of ascorbic acid on CC-derived TECs has also been studied. It is revealed that TECs, which were not treated with ascorbic acid, exhibited poor collagen secretion and thinner tissue structure in vitro. Upon implantation into the defect sites, these TECs failed to fully restore the height of articular cartilage and maintained a slightly weaker cartilage matrix staining, potentially compromising their durability and reparative effects post-implantation. This suggests that TECs without ascorbic acid treatment do not meet the requirements for direct application and therefore, it is necessary to appropriately induce and promote CC-derived TECs in vitro. Ascorbic acid is widely used in scaffold-free cartilage tissue engineering due to its promoting effect on chondrogenic differentiation and extracellular matrix secretion of cartilage cells [50]. The results showed that ascorbic acid upregulated genes related to extracellular matrix production, collagen-related matrix production, and cell adhesion in CC and promoted the secretion of GAG and collagen (Figs. 3 and 4 B, D, E, Fig. 5), which is similar to the results previously reported [51–53]. Apart from its direct role in increasing gene expression, ascorbic acid can also function as a cofactor for prolyl and lysyl hydrolase. The hydroxylation of specific proline and lysine residues within the collagen molecule is essential for collagen cross-linking, a critical process in collagen maturation that plays a significant role in bone and cartilage formation [54,55]. Through RNA-seq analysis of differentially expressed genes, we conducted GO enrichment analysis and discovered that ascorbic acid not only promotes ECM production, binding, and organization in costal chondrocytes, but also enhances cell adhesion (Fig. 4B). Furthermore, ascorbic acid was found to stimulate cellular antioxidant response and inhibit apoptosis in these cells (Fig. 4D). Additionally, we observed that ascorbic acid modulates genes related to fatty acid metabolism in costal chondrocytes (Fig. 4E). Through KEGG pathway enrichment analysis, it was determined that ascorbic acid may exert its regulatory effects through upregulation of the PI3K-Akt and MAPK signaling pathways (Fig. 4E). However, research has found that ascorbic acid also promotes chondrocyte hypertrophy and osteogenic differentiation by upregulating the expression of Runx2, manifested as increased secretion of type I and type X collagen [56–58]. Through mRNA sequencing and qPCR results, it was observed that the expression of the col10 gene in CC did indeed increase. However, based on the results of immunofluorescence staining, both CC-derived TECs with and without ascorbic acid treatment exhibited minimal expression of COLX, with no significant differences observed. This may be attributed to the inherent tendency of CC towards spontaneous hypertrophy, where the effects of ascorbic acid stimulation may be difficult to discern [23].

In this study, CCs were used as the seeding cells for several reasons. Firstly, scaffold-free cartilage tissue engineering needs a great quantity of target cells. Different from articular chondrocytes which are limited in source, CCs can be isolated from costal cartilage, an abundant source of hyaline cartilage storage in the human body [20,23]. Other advantages of CCs over articular chondrocytes include low donor site morbidity, higher initial cell yield and proliferation rate, and better re-differentiation ability [12,13,23]. After two passages of expansion, a biopsy weighing a few milligrams would yield tens of millions of cells, thereby providing a substantial quantity suitable for generating autologous grafts to meet clinical demands [59]. Prior experiments have demonstrated the in vitro capacity of costal chondrocytes to undergo differentiation and acquire an articular chondrocyte phenotype, as evidenced by the secretion of GAGs and type II collagen [13,59,60]. Therefore, CCs have been regarded as a promising alternative for articular chondrocytes. In this study, in the absence of chondrogenic induction conditions, CC-derived TECs still demonstrated the ability of hyaline cartilaginous matrix secretion, as depicted by the histological staining results. The uninduced MSC-derived TEC only exhibited the secretion capability of fibrous cartilage matrix and requires secondary differentiation in vivo, which introduces uncertainty in both differentiation and reparative effects [7,8,61]. Previous experiments have reported that undifferentiated MSCs have inferior regenerative effects after transplantation, thus demonstrating the advantages of CC[62,63]. The results of in vivo repair also demonstrate that CC-derived TECs treated with ascorbic acid exhibited tissue characteristics of mature hyaline cartilage, with staining intensity similar to that of surrounding native cartilage (Figs. 7 and 8).

However, there are still some limitations in this study. Firstly, CCs had a slight tendency to hypertrophy as observed. At least in our experimental results, this trend did not become stronger over time and did not affect the reparative effects of TEC derived from CC on the morphology and structure of articular cartilage. Although the long-term effect of this phenomenon on cartilage repair is unclear, future studies can modify and improve the fabrication procedure to overcome this feature. Additionally, in vivo evaluation in big animal models is needed before CC-derived TECs are ready for clinical translation.

5. Conclusion

In summary, we developed a CC-derived scaffold-free TEC for articular cartilage repair without requiring special culture equipment. The fabricated TECs were first characterized and analyzed for chondrogenesis in vitro. Further in vivo outcomes showed proper cartilage regeneration, subchondral remodeling, and integration into the surrounding native tissue. Therefore, the CC-derived TEC be considered as a promising scaffold-free articular cartilage repair strategy.

Data availability

The datasets used and/or analyzed during the current study are available from the corresponding author upon reasonable request.

Funding

This research was sponsored by the Natural Science Foundation of Shanghai (No.21ZR1448000) and the National Natural Science Foundation of China (No. 81820108020).

Ethical approval

Animal study approved by Animal Care and Use Committee of Shanghai Sixth People's Hospital (No. DWSY2022-0173).

Author contribution statement

All persons who meet authorship criteria are listed as authors, and all authors certify that they have participated sufficiently in the work to take public responsibility for the content, including participation in the concept, design, analysis, writing, or revision of the manuscript. Each author certifies that this material or part thereof has not been published

in another journal, that it is not currently submitted elsewhere, and that it will not be submitted elsewhere until a final decision regarding publication of the manuscript in Journal of Orthopaedic Translation has been made.Indicate the specific contributions made by each author (list the authors' initials followed by their surnames, e.g., Y.L. Cheung). The name of each author must appear at least once in each of the three categories below.

Category 1

Conception and design of study: __D.J. Du__,_C.Q. Zhang_,_K.W. Zheng_acquisition of data: _ K.W. Zheng _,__Y.Y. Ma__,_C. Chiu_,__M.X. Xue__analysis and/or interpretation of data: _ K.W. Zheng _,__Y.Y. Ma__, _C. Chiu_,__M.X. Xue _

Category 2

Drafting the manuscript: __ K.W. Zheng _,__Y.Y. Marevising the manuscript critically for important intellectual content: _ D.J. Du__,_C.Q. Zhang_,_K.W. Zheng_

Category 3

Approval of the version of the manuscript to be published (the names of all authors must be listed):_ K.W. Zheng _,__Y.Y. Ma__,_C. Chiu_,__M.X. Xue,__ C.Q. Zhang __, D.J. Du.

Declaration of competing interest

A conflict of interest occurs when an individual's objectivity is potentially compromised by a desire for financial gain, prominence, professional advancement or a successful outcome. The Editors of the *Journal of Orthopaedic Translation* strive to ensure that what is published in the Journal is as balanced, objective and evidence-based as possible. Since it can be difficult to distinguish between an actual conflict of interest and a perceived conflict of interest, the Journal requires authors to disclose all and any potential conflicts of interest.

Acknowledgements

All persons who have made substantial contributions to the work reported in the manuscript (e.g., technical help, writing and editing assistance, general support), but who do not meet the criteria for authorship, are named in the Acknowledgements and have given us their written permission to be named. If we have not included an Acknowledgements, then that indicates that we have not received substantial contributions from non-authors.

Appendix A. Supplementary data

Supplementary data to this article can be found online at https://doi.org/10.1016/j.jot.2024.02.005.

References

[1] Morouco P, Fernandes C, Lattanzi W. Challenges and innovations in osteochondral regeneration: insights from biology and inputs from bioengineering toward the optimization of tissue engineering strategies. J Funct Biomater 2021;12(1).
[2] Makris EA, Gomoll AH, Malizos KN, Hu JC, Athanasiou KA. Repair and tissue engineering techniques for articular cartilage. Nat Rev Rheumatol 2015;11(1):21–34.
[3] Wei W, Dai H. Articular cartilage and osteochondral tissue engineering techniques: recent advances and challenges. Bioact Mater 2021;6(12):4830–55.
[4] DuRaine GD, Brown WE, Hu JC, Athanasiou KA. Emergence of scaffold-free approaches for tissue engineering musculoskeletal cartilages. Ann Biomed Eng 2015;43(3):543–54.
[5] Athanasiou KA, Eswaramoorthy R, Hadidi P, Hu JC. Self-organization and the self-assembling process in tissue engineering. Annu Rev Biomed Eng 2013;15:115–36.
[6] Cooper SM, Rainbow RS. The developing field of scaffold-free tissue engineering for articular cartilage repair. Tissue Eng Part B Rev; 2021.
[7] Ando W, Tateishi K, Hart DA, Katakai D, Tanaka Y, Nakata K, et al. Cartilage repair using an in vitro generated scaffold-free tissue-engineered construct derived from porcine synovial mesenchymal stem cells. Biomaterials 2007;28(36):5462–70.
[8] Ando W, Tateishi K, Katakai D, Hart DA, Higuchi C, Nakata K, et al. In vitro generation of a scaffold-free tissue-engineered construct (TEC) derived from human synovial mesenchymal stem cells: biological and mechanical properties and further chondrogenic potential. Tissue Eng Part A 2008;14(12):2041–9.
[9] Shimomura K, Yasui Y, Koizumi K, Chijimatsu R, Hart DA, Yonetani Y, et al. First-in-Human pilot study of implantation of a scaffold-free tissue-engineered construct generated from autologous synovial mesenchymal stem cells for repair of knee chondral lesions. Am J Sports Med 2018;46(10):2384–93.
[10] Xiang Y, Bunpetch V, Zhou W, Ouyang H. Optimization strategies for ACI: a step-chronicle review. J Orthop Translat 2019;17:3–14.
[11] Charlier E, Deroyer C, Ciregia F, Malaise O, Neuville S, Plener Z, et al. Chondrocyte dedifferentiation and osteoarthritis (OA). Biochem Pharmacol 2019;165:49–65.
[12] Lee J, Lee E, Kim HY, Son Y. Comparison of articular cartilage with costal cartilage in initial cell yield, degree of dedifferentiation during expansion and redifferentiation capacity. Biotechnol Appl Biochem 2007;48(Pt 3):149–58.
[13] Isogai N, Kusuhara H, Ikada Y, Ohtani H, Jacquet R, Hillyer J, et al. Comparison of different chondrocytes for use in tissue engineering of cartilage model structures. Tissue Eng 2006;12(4):691–703.
[14] El Sayed K, Haisch A, John T, Marzahn U, Lohan A, Muller RD, et al. Heterotopic autologous chondrocyte transplantation–a realistic approach to support articular cartilage repair? Tissue Eng Part B Rev 2010;16(6):603–16.
[15] Chiu C, Zheng K, Xue M, Du D. Comparative analysis of hyaline cartilage characteristics and chondrocyte potential for articular cartilage repair. Ann Biomed Eng 2024. https://doi.org/10.1007/s10439-023-03429-1.
[16] Huwe LW, Brown WE, Hu JC, Athanasiou KA. Characterization of costal cartilage and its suitability as a cell source for articular cartilage tissue engineering. J Tissue Eng Regen Med 2018;12(5):1163–76.
[17] Huwe LW, Sullan GK, Hu JC, Athanasiou KA. Using costal chondrocytes to engineer articular cartilage with applications of passive axial compression and bioactive stimuli. Tissue Eng Part A 2018;24(5–6):516–26.
[18] Johnson TS, Xu JW, Zaporojan VV, Mesa JM, Weinand C, Randolph MA, et al. Integrative repair of cartilage with articular and nonarticular chondrocytes. Tissue Eng 2004;10(9–10):1308–15.
[19] Armiento AR, Alini M, Stoddart MJ. Articular fibrocartilage - why does hyaline cartilage fail to repair? Adv Drug Deliv Rev 2019;146:289–305.
[20] Gao Y, Gao J, Li H, Du D, Jin D, Zheng M, et al. Autologous costal chondral transplantation and costa-derived chondrocyte implantation: emerging surgical techniques. Ther Adv Musculoskelet Dis 2019;11. 1759720X19877131.
[21] Du D, Hsu P, Zhu Z, Zhang C. Current surgical options and innovation for repairing articular cartilage defects in the femoral head. J Orthop Translat 2020;21:122–8.
[22] Ma Y, Zheng K, Pang Y, Xiang F, Gao J, Zhang C, et al. Anti-hypertrophic effect of synovium-derived stromal cells on costal chondrocytes promotes cartilage repairs. Journal of Orthopaedic Translation 2022;32:59–68.
[23] Zheng K, Ma Y, Chiu C, Pang Y, Gao J, Zhang C, et al. Co-culture pellet of human Wharton's jelly mesenchymal stem cells and rat costal chondrocytes as a candidate for articular cartilage regeneration: in vitro and in vivo study. Stem Cell Res Ther 2022;13(1):386.
[24] Weiss-Bilka HE, McGann ME, Meagher MJ, Roeder RK, Wagner DR. Ectopic models for endochondral ossification: comparing pellet and alginate bead culture methods. J Tissue Eng Regen Med 2018;12(1):e541–9.
[25] Babur BK, Ghanavi P, Levett P, Lott WB, Klein T, Cooper-White JJ, et al. The interplay between chondrocyte redifferentiation pellet size and oxygen concentration. PLoS One 2013;8(3):e58865.
[26] Gosset M, Berenbaum F, Thirion S, Jacques C. Primary culture and phenotyping of murine chondrocytes. Nat Protoc 2008;3(8):1253–60.
[27] Liao Y, Long JT, Gallo CJR, Mirando AJ, Hilton MJ. Isolation and culture of murine primary chondrocytes: costal and growth plate cartilage. Methods Mol Biol 2021;2230:415–23.
[28] Shajib MS, Futrega K, Franco RAG, McKenna E, Guillesser B, Klein TJ, et al. Method for manufacture and cryopreservation of cartilage microtissues. J Tissue Eng 2023;14:20417314231176901.
[29] Gupta S, Lin J, Ashby P, Pruitt L. A fiber reinforced poroelastic model of nanoindentation of porcine costal cartilage: a combined experimental and finite element approach. J Mech Behav Biomed Mater 2009;2(4):326–38.
[30] Han L, Reiter MP, Ward SH, Perry B, Mann A, Freeman JW, et al. Intra-articular injection of epigallocatechin (EGCG) crosslinks and alters biomechanical properties of articular cartilage, a study via nanoindentation. PLoS One 2022;17(10):e0276626.
[31] van den Borne MP, Raijmakers NJ, Vanlauwe J, Victor J, de Jong SN, Bellemans J, et al. International cartilage repair society (ICRS) and oswestry macroscopic cartilage evaluation scores validated for use in autologous chondrocyte implantation (ACI) and microfracture. Osteoarthritis Cartilage 2007;15(12):1397–402.
[32] Mainil-Varlet P, Aigner T, Brittberg M, Bullough P, Hollander A, Hunziker E, et al. Histological assessment of cartilage repair: a report by the histology endpoint committee of the international cartilage repair society (ICRS). J Bone Joint Surg Am 2003;85-A(Suppl 2):45–57.
[33] Orth P, Madry H. Complex and elementary histological scoring systems for articular cartilage repair. Histol Histopathol 2015;30(8):911–9.
[34] Yasui Y, Ando W, Shimomura K, Koizumi K, Ryota C, Hamamoto S, et al. Scaffold-free, stem cell-based cartilage repair. J Clin Orthop Trauma 2016;7(3):157–63.

[35] Stuart MP, Matsui RAM, Santos MFS, Cortes I, Azevedo MS, Silva KR, et al. Successful low-cost scaffold-free cartilage tissue engineering using human cartilage progenitor cell spheroids formed by micromolded nonadhesive hydrogel. Stem Cell Int 2017;2017:7053465.
[36] Velasco MA, Narvaez-Tovar CA, Garzon-Alvarado DA. Design, materials, and mechanobiology of biodegradable scaffolds for bone tissue engineering. BioMed Res Int 2015;2015:729076.
[37] Ovsianikov A, Khademhosseini A, Mironov V. The synergy of scaffold-based and scaffold-free tissue engineering strategies. Trends Biotechnol 2018;36(4):348–57.
[38] Lee SY, Lee JW. 3D spheroid cultures of stem cells and exosome applications for cartilage repair. Life 2022;12(7).
[39] Chaicharoenaudomrung N, Kunhorm P, Noisa P. Three-dimensional cell culture systems as an in vitro platform for cancer and stem cell modeling. World J Stem Cell 2019;11(12):1065–83.
[40] Sun K, Tao C, Wang DA. Scaffold-free approaches for the fabrication of engineered articular cartilage tissue. Biomed Mater 2022;17(2).
[41] Shajib MS, Futrega K, Jacob Klein T, Crawford RW, Doran MR. Collagenase treatment appears to improve cartilage tissue integration but damage to collagen networks is likely permanent. J Tissue Eng 2022;13:20417314221074207.
[42] Thorp H, Kim K, Kondo M, Grainger DW, Okano T. Fabrication of hyaline-like cartilage constructs using mesenchymal stem cell sheets. Sci Rep 2020;10(1):20869.
[43] Yanase M, Ikeda H, Matsui A, Maekawa H, Noiri E, Tomiya T, et al. Lysophosphatidic acid enhances collagen gel contraction by hepatic stellate cells: association with rho-kinase. Biochem Biophys Res Commun 2000;277(1):72–8.
[44] Lu Y, Zhang W, Wang J, Yang G, Yin S, Tang T, et al. Recent advances in cell sheet technology for bone and cartilage regeneration: from preparation to application. Int J Oral Sci 2019;11(2):17.
[45] Sha'ban M, Ahmad Radzi MA. Scaffolds for cartilage regeneration: to use or not to use? Adv Exp Med Biol 2020;1249:97–114.
[46] Huey DJ, Hu JC, Athanasiou KA. Unlike bone, cartilage regeneration remains elusive. Science 2012;338(6109):917–21.
[47] van de Breevaart Bravenboer J, In der Maur CD, Bos PK, Feenstra L, Verhaar JA, Weinans H, et al. Improved cartilage integration and interfacial strength after enzymatic treatment in a cartilage transplantation model. Arthritis Res Ther 2004;6(5):R469–76.
[48] Englert C, McGowan KB, Klein TJ, Giurea A, Schumacher BL, Sah RL. Inhibition of integrative cartilage repair by proteoglycan 4 in synovial fluid. Arthritis Rheum 2005;52(4):1091–9.
[49] Fujie H, Nansai R, Ando W, Shimomura K, Moriguchi Y, Hart DA, et al. Zone-specific integrated cartilage repair using a scaffold-free tissue engineered construct derived from allogenic synovial mesenchymal stem cells: biomechanical and histological assessments. J Biomech 2015;48(15):4101–8.
[50] Li T, Liu B, Chen K, Lou Y, Jiang Y, Zhang D. Small molecule compounds promote the proliferation of chondrocytes and chondrogenic differentiation of stem cells in cartilage tissue engineering. Biomed Pharmacother 2020;131:110652.
[51] Asnaghi MA, Duhr R, Quasnichka H, Hollander AP, Kafienah W, Martin I, et al. Chondrogenic differentiation of human chondrocytes cultured in the absence of ascorbic acid. J Tissue Eng Regen Med 2018;12(6):1402–11.
[52] Temu TM, Wu KY, Gruppuso PA, Phornphutkul C. The mechanism of ascorbic acid-induced differentiation of ATDC5 chondrogenic cells. Am J Physiol Endocrinol Metab 2010;299(2):E325–34.
[53] Clark AG, Rohrbaugh AL, Otterness I, Kraus VB. The effects of ascorbic acid on cartilage metabolism in Guinea pig articular cartilage explants. Matrix Biol 2002;21(2):175–84.
[54] Lindsey RC, Cheng S, Mohan S. Vitamin C effects on 5-hydroxymethylcytosine and gene expression in osteoblasts and chondrocytes: potential involvement of PHD2. PLoS One 2019;14(8):e0220653.
[55] D'Aniello C, Cermola F, Patriarca EJ, Minchiotti G. Vitamin C in stem cell biology: impact on extracellular matrix homeostasis and epigenetics. Stem Cell Int 2017;2017:8936156.
[56] Langenbach F, Handschel J. Effects of dexamethasone, ascorbic acid and β-glycerophosphate on the osteogenic differentiation of stem cells in vitro. Stem Cell Res Ther 2013;4(5):117.
[57] Farquharson C, Berry JL, Barbara Mawer E, Seawright E, Whitehead CC. Ascorbic acid-induced chondrocyte terminal differentiation: the role of the extracellular matrix and 1,25-dihydroxyvitamin D. Eur J Cell Biol 1998;76(2):110–8.
[58] Nishimori S, Lai F, Shiraishi M, Kobayashi T, Kozhemyakina E, Yao TP, et al. PTHrP targets HDAC4 and HDAC5 to repress chondrocyte hypertrophy. JCI Insight 2019;4(5).
[59] Tay AG, Farhadi J, Suetterlin R, Pierer G, Heberer M, Martin I. Cell yield, proliferation, and postexpansion differentiation capacity of human ear, nasal, and rib chondrocytes. Tissue Eng 2004;10(5–6):762–70.
[60] Murphy MK, DuRaine GD, Reddi A, Hu JC, Athanasiou KA. Inducing articular cartilage phenotype in costochondral cells. Arthritis Res Ther 2013;15(6):R214.
[61] Shimomura K, Ando W, Tateishi K, Nansai R, Fujie H, Hart DA, et al. The influence of skeletal maturity on allogenic synovial mesenchymal stem cell-based repair of cartilage in a large animal model. Biomaterials 2010;31(31):8004–11.
[62] Wu Y, Yang Z, Denslin V, Ren X, Lee CS, Yap FL, et al. Repair of osteochondral defects with predifferentiated mesenchymal stem cells of distinct phenotypic character derived from a nanotopographic platform. Am J Sports Med 2020;48(7):1735–47.
[63] Yoon Y, Khan IU, Choi KU, Jung T, Jo K, Lee SH, et al. Different bone healing effects of undifferentiated and osteogenic differentiated mesenchymal stromal cell sheets in canine radial fracture model. Tissue Eng Regen Med 2018;15(1):115–24.